Scattering from a Round Metal Post and Gap

JOHN A. BRADSHAW

Abstract—**Improved expressions are derived for the microwave fields scattered by a uniform electric-field incident on and parallel to a round metal post, with gap, in waveguide and in two related structures. A pair of variational expressions are found for the scattering and for the gap reactance under even excitation. The results are compared with those due to Lewin, and with data in the *Waveguide Handbook*.**

I. Introduction

A MICROWAVE structure of current interest is the round metal post, extending partway across a rectangular waveguide, its axis parallel to the E lines of the propagating mode. An open gap will be assumed between the post and the floor of the guide, although in practice this gap often contains a passive or active semiconductor. The structure was analyzed by Infeld in 1949 [1] and by Lewin in 1951 [2], 1957 [3], and 1959 [4]. Certain shortcomings in Lewin's papers triggered the present work which, although critical of these papers, builds in large part on Lewin's pioneering efforts.

We will emphasize the field aspects of scattering from a passive loss-free (PLF) post and gap. The unexpected clarity of the results makes a comparison with Marcuvitz's data [5] useful. In a companion paper we will derive the gap impedance seen by a driven post [6], as recently measured by Eisenhart and Khan [7]. These authors take a flat strip as a model for their post; we will, instead, first remove the sidewalls of the guide to simplify the analysis of scattering by a *round* post, and later account for the sidewalls by image methods.

II. An Outline of the Analysis

Our first model, sketched in Fig. 1, assumes infinite parallel metal plates separated by a distance b. A metal post of radius a and ideal conductivity extends down from $y=b$ to $y=d$ along the axis of a cylindrical coordinate system $(r\theta y)$, leaving a gap between $y=d$ and the origin in the lower plate. The odd system $(r\theta y)$ was chosen so y fits later into the (xyz) system of a rectangular waveguide. In this model a plane TEM wave $\sim$ Re $[\exp j(\omega t-kz)]$ falls on the post, causing currents along its surface and excess charge near the gap. The currents and charge cause scattering fields; of these, the TEM alone reaches large values of r, if, as we usually assume, $b<\lambda/2$.

If the post had no gap, an expansion about the post axis,

$$\exp(-jkz) = J_0(kr) + 2\sum_{m=1}^{\infty}(-j)^m J_m(kr)\cos m\theta \quad (1)$$

would lead to the classical formula for power scattered per unit incident intensity: the total scattering cross section is a sum of distinct contributions from each $m\theta$ mode,

$$Qb = \frac{4b}{k}\sum_{m=0}^{\infty}\epsilon_m \sin^2\delta_m. \quad (2)$$

Here the phase angles δ_m are those of the Hankel function of the second kind, $H_m(ka)$, and $\epsilon_m = 2-\delta_m{}^0$. (We will omit the superscript from H_m; $\cot\delta_m = -N_m(ka)/J_m(ka)$ is the notation of Morse and Feshbach [8, p. 1564].) The first three contributions to Qb are plotted as functions of ka in Fig. 2. The extra curves $\sin\delta_m'$ refer to scattering from waves with electric polarization across the post, and were drawn to reassure the reader that such may be ignored. The major interest lies in curves of $\sin\delta_0$ and $\sin\delta_1$; introducing a gap will not disturb the relative amplitudes scattered from a post excited by a plane traveling wave.

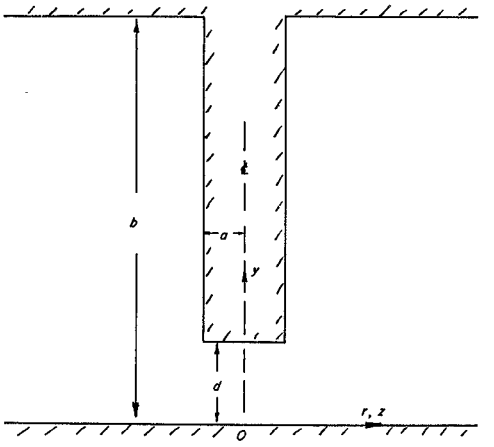

Fig. 1. The post with gap, between parallel plates, with the dimensions a, b, and d, and the coordinates r, y, and z of the systems $(r\theta y)$ and (xyz).

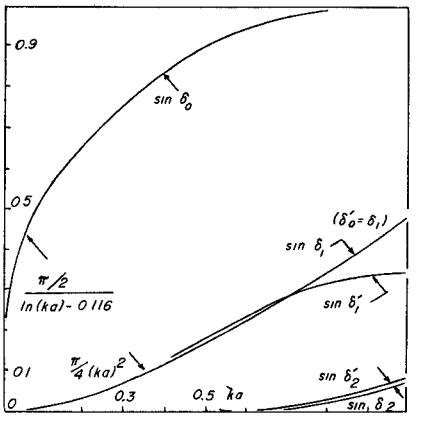

Fig. 2. The scattering amplitudes, $\sin\delta_m$, of modes of a round cylinder of radius a, under excitation by a plane traveling wave $\sim$ Re $[\exp -jkz]$ are plotted against ka.

Manuscript received September 22, 1971; revised December 7, 1972.
The author is with the Electrophysics Division, Rensselaer Polytechnic Institute, Troy, N. Y. 12181.

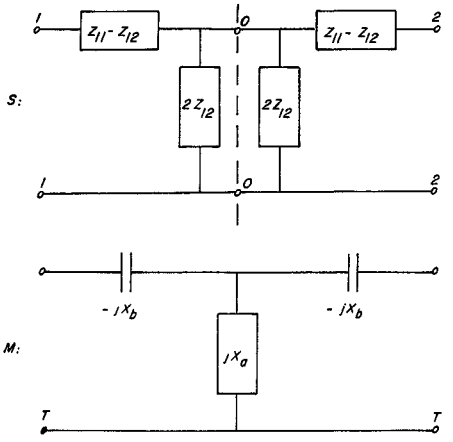

Fig. 3. The equivalent T circuits of a post in waveguide, following Schwinger (S) and Marcuvitz (M).

The relative scattered amplitudes depend, however, on the type of excitation: in the presence of a second (reversed) traveling wave $\sim$ Re $[\exp j(\omega t+kz)]$, the net excitation will include a standing wave. Schwinger [9] based his analysis of scatter from a solid post on even and odd standing-wave fields, cos kz and sin kz, respectively, which excite even and odd m-terms in Qb. He related the scatter to elements of a T circuit, S in Fig. 3; Marcuvitz's data on the post with gap are in terms of X_a and X_b, the lumped shunt and series reactance of his T circuit, M in Fig. 3. To compare them, the impedance across the 1,1 terminals of Schwinger's circuit, under an even excitation which produces an open circuit across the 0,0 terminals, is $Z_{11}+Z_{12}=j(2X_a-X_b)$. The 1,1 impedance under odd excitation, which produces a short across 0,0 terminals, is $Z_{11}-Z_{12}=-jX_b$.

In the data for small gaps, X_b with increasing post radius follows the sin δ_1 curve of Fig. 2. The data appear in three sets: $ka \triangleq 0.15$ for set I, ka(II) $\triangleq 0.30$, and ka(III) $\triangleq 0.60$. The ratio (sin δ_0/sin δ_1) for these sets is close to 28, 12, and 4, respectively. The present paper considers only scatter independent of θ, so at least in the third set we must treat X_b with some care.

In our analysis, two different routes lead from Maxwell's relations to formulas for modal impedances Z_n. [The Z_n are ratios of Fourier amplitudes in expressions for $\epsilon(y)$, the electric field at the post radius, and $I(y)$, the post current.] In an example, we will use relations between ϵ and I to refine both functions of y well beyond zero order, where ϵ is assumed uniform in the gap. From ϵ and I we will find S, the ratio of scattered to incident TEM components of the electric field. Again two routes, one direct and one variational, lead to formulas for $S(kb, a, d)$.

An S may also be found for a post in rectangular waveguide, or for a comb structure in stripline [10], and related to parameters of the equivalent T circuit. After analysis of Marcuvitz's data in terms of this S and the gap capacitive reactance X_c, we will review briefly some other literature on these structures. We turn now to work, through the model of an isolated post, toward results that will apply in waveguide.

III. Fields and Z_n by Green's Function Methods

A brief sketch below of the theory will serve to define our notation; the major symbols are also listed in Appendix I. The surface density of current excited on the post, $J_y(r\theta y) = I(y)\delta(r-a)/2\pi a$, is the source of a scattered wave of vector potential A_y satisfying $[\nabla^2+k^2]A_y=-\mu J_y$. We will ignore some details of the gap, including any radial currents there. With Green's second theorem one finds $A_y=\mu\iiint_v GJ_y\,dv'$ + a surface integral. In this form, v is the volume $\{0<y<b,\ 0<r<R\}$ in a large cylinder around the post, and G is the (yy) term of a dyadic Green's function [11]. We can treat G here as a scalar. The surface integral vanishes by reason of a radiation condition at $r=R$, and because the normal derivatives of G and of A_y vanish on the metal plates at $y=0$ and $y=b$ [12].

The complete expression for G satisfies $[\nabla^2+k^2]G=-\delta(\vec{x}-\vec{x}')$, and appears in Appendix II. The part of G independent of θ is

$$G_0(r, r'; y, y') = -jH_0(kr>)J_0(kr<)[(4b)^{-1}] + \sum_{n=1}^{\infty} K_0(\Gamma_{n0}r>)I_0(\Gamma_{n0}r<)[(\pi b)^{-1}] \cdot \cos n\pi y'/b \cos n\pi y/b. \quad (3)$$

Here H_0 is the Hankel function, J_0 is the Bessel function, K_0 and I_0 are modified Bessel functions, $r<$ represents the radial position of the source point $\vec{x}'$, and $r>$ represents the position of the observer at $\vec{x}$. We assume $b<\lambda/2$ so that $\Gamma_{n0}^2\equiv(n\pi/b)^2-k^2$ is positive for $n\geq 1$. To emphasize dependence on r or a, in this section and the next, the arguments of J_0 and $H_0(kr$ or $ka)$, and of K_0 and $I_0(\Gamma_{n0}r$ or $\Gamma_{n0}a)$, will be written (r) or (a). Writing $I(y)$ as a Fourier cosine series in $0<y<b$, thus $I(y)=I_0+2\sum_{n=1}^{\infty} I_n \cos n\pi y/b$, one can integrate formally over GI to obtain A_y for $r>a$:

$$A_y = \frac{-j\mu}{4} I_0H_0(r)J_0(a) + \frac{\mu}{\pi}\sum_{n=1}^{\infty} K_0(r)I_0(a)I_n \cos n\pi y/b. \quad (4)$$

From here on $\pi y/b$ will usually be shortened to $\bar{u}$.

The scattered fields derived from A_y have three vector components:

$$E_y^s = -j\omega\left[1+\frac{1}{k^2}\frac{\partial^2}{\partial y^2}\right]A_y$$

$$E_r^s = -j\frac{\omega}{k^2}\frac{\partial^2}{\partial r\partial y}A_y$$

$$\mu H_\theta^s = -\frac{\partial}{\partial r}A_y. \quad (5)$$

We will omit E_r^s; writing dK_0/dq as $K_0'(q)$, we find for E_y^s and H_θ^s:

$$E_y^s = -\frac{\omega\mu}{4} I_0H_0(r)J_0(a) + \frac{j\omega\mu}{\pi}\sum_{n=1}^{\infty} I_nK_0(r)I_0(a)\cos n\bar{u}\frac{\Gamma_{n0}^2}{k^2} \quad (6)$$

$$H_\theta^s = \frac{jk}{4} I_0H_0'(r)J_0(a) - \frac{1}{\pi}\sum_{n=1}^{\infty} I_nK_0'(r)I_0(a)\cos n\bar{u}\Gamma_{n0}. \quad (7)$$

At $r=a$, both in the gap and along the surface of the post, one can assume a second Fourier cosine series to represent the

total y-component of electric field: $\epsilon(y)=\epsilon_0{}^t+2\sum_{n=1}^{\infty}\epsilon_n\cos n\bar{u}$. This total field may include both incident and scattered elements, $\epsilon^t=\epsilon^i+\epsilon^s$; in (6) we can find $\epsilon^s=E_y{}^s(r=a)$. Now comparing Fourier coefficients leads us to define the modal impedances mentioned previously:

$$Z_0I_0\equiv-\epsilon_0{}^sb,\quad Z_0=\frac{\zeta kb}{4}H_0(ka)J_0(ka) \tag{8}$$

$$Z_nI_n\equiv-\epsilon_nb,\quad Z_n=-\frac{j\zeta kb}{2\pi}K_0(\Gamma_{n0}a)I_0(\Gamma_{n0}a)\Gamma_{n0}{}^2[k^{-2}]. \tag{9}$$

Lewin's result by this method, his equation for Z_n, is [3, eq. 10]:

$$-2jX_n=-\frac{j\zeta kb}{2\pi}K_0(\Gamma_{n0}a)\Gamma_{n0}{}^2[k^{-2}]. \tag{10}$$

He also anticipated a factor $\exp(n\pi a/b)$, but did not give $I_0(\Gamma_{n0}a)$. In these formulas $\zeta=1/\eta$ is the usual impedance of free space $\sqrt{\mu/\epsilon}$.

IV. Fields and Z_n by a Direct Match

To confirm the results above, one can find modal admittances, inverses to Z_0 and Z_n, by a complementary approach suggested in Lewin's 1959 paper [4]. $E_y{}^s$, as a solution of the wave equation outside its source, the current cylinder at $r=a$, must have the form

$$E_y{}^s=\epsilon_0{}^s\frac{H_0(r)}{H_0(a)}+2\sum_{n=1}^{\infty}\epsilon_n\frac{K_0(r)}{K_0(a)}\cos n\bar{u}. \tag{11}$$

The corresponding trial forms for $E_r{}^s$ and $H_\theta{}^s$ must satisfy

$$\frac{\partial E_y{}^s}{\partial y}+\frac{1}{r}\frac{\partial rE_r{}^s}{\partial r}=0$$

$$\frac{\partial E_r{}^s}{\partial y}-\frac{\partial E_y{}^s}{\partial r}=-j\omega\mu H_\theta{}^s. \tag{12}$$

Hence, again omitting $E_r{}^s$, we find

$$H_\theta{}^s=-j\eta\epsilon_0{}^s\frac{H_0'(r)}{H_0(a)}+2jk\eta\sum_{n=1}^{\infty}\frac{\epsilon_n}{\Gamma_{n0}}\frac{K_0'(r)}{K_0(a)}\cos n\bar{u}. \tag{13}$$

In the gap and inside the current cylinder, the matching trial forms must be well-behaved at $r=0$ and must satisfy the wave equation. $E_y{}^s$ must be continuous across $r=a$, but $H_\theta{}^s$ will be discontinuous by the amplitude of the y-directed current:

$$E_y{}^s=\epsilon_0{}^s\frac{J_0(r)}{J_0(a)}+2\sum_{n=1}^{\infty}\epsilon_n\frac{I_0(r)}{I_0(a)}\cos n\bar{u} \tag{14}$$

$$H_\theta{}^s=-j\epsilon_0{}^s\eta\frac{J_0'(r)}{J_0(a)}+2j\eta\sum_{n=1}^{\infty}\epsilon_n\frac{I_0'(r)}{I_0(a)}\cos n\bar{u}\frac{k}{\Gamma_{n0}} \tag{15}$$

$$I(y)=2\pi a\Delta H_\theta{}^s(r=a)=-j\eta\epsilon_0{}^s\left\{\frac{-2j}{\pi ka}\right\}\frac{2\pi a}{H_0(a)J_0(a)}$$

$$+2j\eta\sum_{n=1}^{\infty}\epsilon_n\frac{2\pi a}{K_0(a)I_0(a)}\frac{k}{\Gamma_{n0}}\left\{\frac{-1}{\Gamma_{n0}a}\right\}\cos n\bar{u}. \tag{16}$$

Here the terms in brackets represent the Wronskians $\{H_0, J_0\}$ and $\{K_0, I_0\}$. The desired modal admittances, defined by $I_0=-Y_0\epsilon_0{}^sb$ and by $I_n=-Y_n\epsilon_nb$, can be identified in (16).

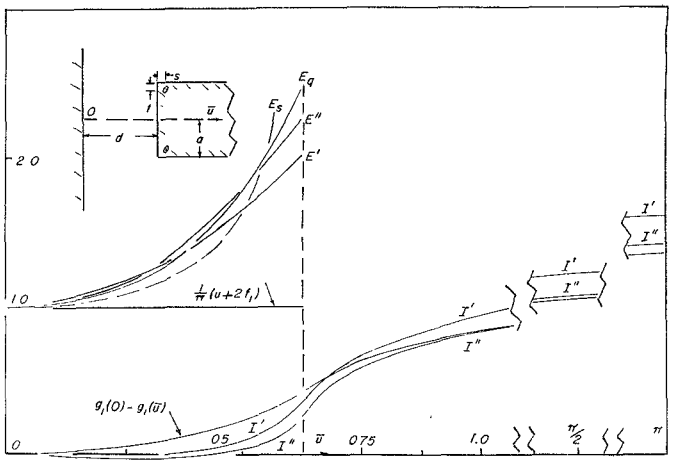

Fig. 4. Trial forms for $\epsilon(y)$, the gap field, and the corresponding forms for the post current $I(y)$ are plotted against $\bar{u}=\pi y/b$, with the gap parameter $u=\pi d/b$ taken as 5/8.

Comparing them with (8) and (9), one finds, indeed, $Y_0=1/Z_0$ and $Y_n=1/Z_n$. Lewin's result by this method is in [4, eq. 5]:

$$Y_n=4\pi\eta j\frac{ka}{\Gamma_{n0}b}\frac{K_0'(\Gamma_{n0}a)}{K_0(\Gamma_{n0}a)}. \tag{17}$$

Lewin omitted the fields inside the post and missed the correction $-I_0'/I_0$ which, with K_0'/K_0, gives the Wronskian and aligns the forms in (16) with those in (8) and (9). In our view [13], the incident field $E_y{}^{\text{inc}}=E_y{}^i\exp(-jkz)$ passes *through* the post and gap; the scattered fields inside the post radius are included in the Green's function and are required in this boundary-matching method too.

V. An Example Using the Interrelation of $I(y)$ and $\epsilon(y)$

For a PLF scatterer, we require $\epsilon^t(y)=0$ on the post $(d<y<b)$, and $I(y)=0$ in the gap $(0<y<d)$, so the integral of their product vanishes: $\int_0^b\epsilon(y)I(y)\,dy=0$. First a direct approach will show how the form of $\epsilon(y)$ in the gap affects the form of $I(y)$, and through I, S. Later we will determine S by variation of the integral.

The direct route is smoothed by use of functions related to Clausen's integral [14]. Starting this route, we represent $\epsilon(y)$ in $(0<y<b)$ by a product of a unit step function $h(d-y)$ with a power series in $\bar{u}$ (here $h=1$ if $y<d$, $h=0$ if $y>d$). We next express each term of $\epsilon(y)$ by a Fourier cosine series f_i. The nth coefficient in such cosine series, when multiplied by Y_n, becomes, as we have seen, the nth coefficient in the corresponding cosine series g_i for $I(y)$. Then the weight of each power of $\bar{u}$ in $\epsilon(y)$ is, with I_0, adjusted so that $I(y)$ vanishes in the gap. Two observations simplify this process. First we note that $K_0(X)\,I_0(X)=1/(2X)$ to within 0.6 percent if $\Gamma_{n0}a=X>5$, within 4 percent if $X>2$, and exactly near $X=\frac{1}{2}$. The relation is of no use below $X=0.4$, but where it applies we may write

$$Y_n\triangleq 4\pi\eta jka^2/Xb\qquad\text{or if } X\triangleq n\pi a/b,\quad Y_n\triangleq 4j\eta ka/n. \tag{18}$$

Secondly, we note that dividing each Fourier coefficient in f_i by n yields a form g_i which readily converts back to a short Clausen series in powers of $\bar{u}$.

The example in Fig. 4 shows three steps in the process of improving $\epsilon(y)$ through $I(y)$; in it we take $u=\pi d/b$, the gap parameter, as $\frac{5}{8}=u$. The three trial forms were the uniform

field $\epsilon(y)=E_0h(d-y)$, and $\epsilon'(y)=E_0h(d-y)(1+a\bar{u}^2/\pi^2)$, and finally, with two adjustable coefficients, $\epsilon''(y)=E_0h(d-y)(1+b\bar{u}/\pi+c\bar{u}^2/\pi^2)$. The choices plotted are $a=1$ for ϵ', and $b=0.28$ and $c=0.69$ for ϵ''. The explicit forms for f_i and g_i, and a figure illustrating these forms for $i=1$, 2, 3, and $u=\frac{5}{8}$, have been retired to Appendix III. In Fig. 4, with the uniform field ϵ, $I(y)$ is zero at $\bar{u}=0$, but increases as $g_1(0)-g_1(\bar{u})$ across the gap; with ϵ', I' in the gap has a second zero; I'' presents a further improvement, and the process could be carried to higher powers of $\bar{u}$ in $\epsilon(y)$ as in minimum-ripple filter design.

The curve E_q in Fig. 4 is a static $E_y(y)$, calculated at $r=a$ for a charged ring at $y=(d+s)$, with ring radius $r=(a-t)$ and with $s=t=a/4$. It represents the effects of rounding the post edge. The dashed curve E_s, for comparison with ϵ' and ϵ'', represents Schwinger's field [9] in the plane of a capacitive iris, and is more singular at $\bar{u}=u$ than those we should consider.

The exact contour of the post end near $y=d$ will affect $I(y)$ and $\epsilon(y)$ there; given a detailed model one might formulate a precise edge condition as required in Wiener–Hopf techniques. The oscillations (Gibbs phenomenon) which the Fourier series for f_1 develops at $y=d$ should be mentioned. Finally, the coefficients a, b, c in the trial forms of $\epsilon(y)$ were assumed to be real; however, these will be complex if modes others than TEM propagate ($b>\lambda/2$). Then ϵ and I may change shape within each cycle, as is the case for $I(y)$ on the linear antenna [15].

VI. A Direct Solution for S

Fine details of the post end should have less effect on S than on $\epsilon(y)$. Since $I_0=-Y_0\epsilon_0{}^ibS$ and $\epsilon_0{}^t=\epsilon_0{}^i(1+S)$ the condition $I(0)=0=I_0+2\sum_{n=1}^{\infty}I_n$ yields an equation for $S\equiv\epsilon_0{}^s/\epsilon_0{}^i$:

$$SY_0+8jka\eta(1+S)q(u)=0. \tag{19}$$

Here, if we may use $Y_n\triangleq 4jka\eta/n$, the real function $q(u)$ is linear in g_i; in zero order it is simply $g_1(0)/u$, and in general through Clausen's series $q(u)$ can be put in the form:

$$q(u)=A_0-\ln|u|+A_2u^2/72+\cdots. \tag{20}$$

The constants A_0 and A_2, evaluated with formulas from Appendix III for the trial curves ϵ, ϵ', and ϵ'' of Fig. 4, yield the the values $A_0=1$, 0.833, 0.877, and $A_2=1$, 1.20, 1.15, respectively. Thus A_0 and A_2 depend little on the coefficients a, b, c, and the main term, $-\ln|u|$, at small u is independent of them. For comparison, Schwinger's direct solution for the capacitive iris is:

$$q(u)=\ln\csc u/2=0.693-\ln|u|+u^2/24+\cdots.$$

To examine the solution for S, we rewrite the complex equation (19) as two real equations with $S=s+jt$. We find

$$s^2+t^2+s+t\cot\delta_0=0 \tag{21}$$

$$s=t(8ka\eta|Z_0|\csc\delta_0q(u)-\cot\delta_0). \tag{22}$$

The first equation defines a circle on the complex S plane, which passes through the points $S=0$ and $S=-1$, with center at $S=-\frac{1}{2}[1+j\cot\delta_0]$ and radius $\frac{1}{2}\csc\delta_0$. The circle thus depends on ka, but not on $q(u)$ or on the gap d. Its intersection with the line through the origin given by (22) defines the complex scattering S for a given post and frequency.

VII. Variational Expressions for S

S may also be found from integrals in forms which reduce the effects in S of "errors" in $\epsilon(y)$ or $I(y)$. Let us denote by $e(y)$ and $i(y)$ the sums ($n\geq 1$) in the cosine expansions of ϵ and I:

$$e(y)=2\sum_{n=1}^{\infty}\epsilon_n\cos n\bar{u}=\epsilon(y)-\epsilon_0{}^t$$

$$i(y)=2\sum_{n=2}^{\infty}I_n\cos n\bar{u}. \tag{23}$$

The Maxwellian conditions relating $e(y)$ and $i(y)$ in (6) and (16) can be incorporated in two kernels which are real, symmetric in (y, y'), and orthogonal to 1 in the interval $(0<y<b)$. With them we write the parallel forms:

$$e(y)=-j\int_0^b k(y,y';Z)i(y')\,dy'$$

$$=-j\int_0^b k(y,y';Z)I(y')\,dy' \tag{24}$$

$$i(y)=j\int_0^b k(y,y';Y)e(y')\,dy'$$

$$=j\int_0^b k(y,y';Y)\epsilon(y')\,dy'. \tag{25}$$

Here the kernel $k(Z)$ depends on the modal impedances Z_n defined in (9), and the kernel $k(Y)$ depends on Y_n. The second form in each case following is a closed form, but it depends on the approximation from (18), $Y_n{}^a=4jka\eta/n$:

$$k(y,y';Z)=\frac{2j}{b^2}\sum_{n=1}^{\infty}Z_n\cos n\pi y/b\cos n\pi y'/b$$

$$=\frac{\zeta}{8ka}\left[\left(1-\cos\frac{\pi}{b}(y'+y)\right)^{-1}+\left(1-\cos\frac{\pi}{b}(y'-y)\right)^{-1}\right] \tag{26}$$

$$k(y,y';Y)=-2j\sum_{n=1}^{\infty}Y_n\cos n\pi y/b\cos n\pi y'/b$$

$$=-4ka\eta[\ln 2|\cos\pi y/b-\cos\pi y'/b|]. \tag{27}$$

The relation $\int_0^b\epsilon(y)\,I(y)\,dy=0$ now has two forms which the reader will recognize as "variational." To bring this out let us define $\mathcal{Y}=(Y_0S)/(1+S)$ and its inverse $\mathcal{Z}=Z_0(1+S)/S$ so that $\epsilon_0{}^tbI_0=j\mathcal{Y}[\int_0^b\epsilon\,dy]^2=j\mathcal{Z}[\int_0^b I\,dy]^2$. But $\epsilon_0{}^tbI_0=-\int_0^b e(y)\,i(y)\,dy$, so:

$$\epsilon_0{}^tbI_0=j\int_0^b\int_0^b I(y)I(y')k(y,y';Z)\,dydy' \tag{28}$$

$$=-j\int_0^b\int_0^b\epsilon(y)\epsilon(y')k(y,y';Y)\,dydy'. \tag{29}$$

Thus (28) is stationary in $\mathcal{Z}$ for small departures δI from the true current form, provided δI vanishes, like the true I_e, in the gap; and (29) is stationary in $\mathcal{Y}$ for small departures $\delta\epsilon$

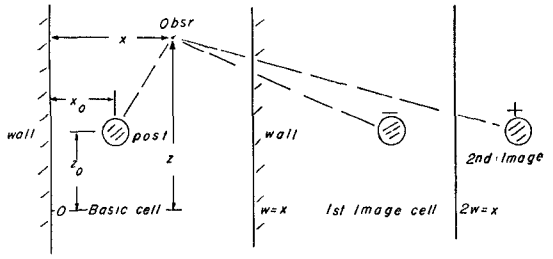

Fig. 5. A post at (x_0, z_0) as seen from above in a waveguide of width w, and the image posts at $x = \pm x_0 + 2w$.

from an exact $\epsilon_e(y)$, if $\delta\epsilon = 0$ on the post. Completing the integrals, we find two forms for S:

$$\mathcal{Y} = -2\sum_{n=1}^{\infty} \epsilon_n{}^2 Y_n[\epsilon_0{}^t]^{-2} = -8jka\eta q(u) = \frac{Y_0 S}{1+S} \quad (30)$$

$$\mathcal{Z} = -2\sum_{n=1}^{\infty} I_n{}^2 Z_n[I_0]^{-2} = +j\zeta[8kaq(u)]^{-1}. \quad (31)$$

The first form suggests a model for $\mathcal{Y}$: a parallel connection of modal admittances seen through transformers with turns ratios $\epsilon_n/\epsilon_0{}^t$. The second form suggests a model for $\mathcal{Z}$: a series connection of modal impedances seen through transformers with turns ratios I_n/I_0. The choice of circuit model depends mainly on whether one knows, or can guess, more about $\epsilon(y)$ or $I(y)$.

Equation (30), with the form of $\epsilon(y)$ used in Fig. 4, yields for $q(u)$ the same expansion given in (20), but with $A_0 = 0.807$, 0.790, 0.820 and $A_2 = 2.00$, 2.34, 2.40 for ϵ, ϵ', and ϵ'', respectively. Again, the main term for small u is $-\ln|u|$, independent of the coefficients a, b, c; A_0 and A_2 do not change much either as $\epsilon(y)$ improves.

VIII. Scattering in Rectangular Guide and in Stripline

These results may now be applied to more practical cases of scattering from a post with gap. The sidewalls of a waveguide, at $x = 0$ and $x = w$ as sketched in Fig. 5, are mirrors for a single post with axis at x_0, z_0. If m is any integer in $(-\infty, \infty)$, the image posts at $x = x_0 + 2mw$ carry currents $I(y)$, while image posts at $x = -x_0 + 2mw$ carry $-I(y)$. In a stripline crossed by a comb structure, each combtooth or post in a lattice of cell width w will carry the same current $I(y)$; in a regular comb, $x_0 = w/2$ [10]. In both guide and stripline, Green's functions may take the form of sums over these replicated sources. Poisson's formula, as given in Appendix IV, converts sums on H_0 and on K_0 to sums on sinusoids. We use it with the $n = 0$ (H_0) sum, but it is both convenient and reasonably accurate[1] to retain in our Green's functions only the nearest, or actual post, as the source of terms for $n \geq 1$. The $G(n)$ following appeared already in (3):

$$G(n) \equiv \sum_{n=1}^{\infty} K_0(\Gamma_{n0}r) I_0(\Gamma_{n0}a)(\pi b)^{-1} \cos n\pi y'/b \cdot \cos n\pi y/b. \quad (32)$$

For waveguide (wg) and stripline (sl), with $\mathcal{K}^2 \equiv k^2 - (\pi/w)^2$, and $\Gamma_{0m}{}^2 \equiv (m\pi/w)^2 - k^2$, where $m \geq 2$, from Appendix IV we find

$$G(wg) = \frac{J_0(ka)}{bw}\left\{\frac{\exp -j\mathcal{K}|z-z_0|}{j\mathcal{K}} \sin \pi x/w \sin \pi x_0/w + \sum_{m=2}^{\infty} \frac{\exp -\Gamma_{0m}|z-z_0|}{\Gamma_{0m}} \sin m\pi x/w \sin m\pi x_0/w\right\} + G(n) \quad (33)$$

$$G(sl) = \frac{J_0(ka)}{bw}\left\{\frac{\exp -jk|z-z_0|}{2jk} + \sum_{m=1}^{\infty} \frac{\exp -\Gamma_{0m}|z-z_0|}{\Gamma_{0m}} \cos m\pi x/w \cos m\pi x_0/w\right\} + G(n). \quad (34)$$

These two Green's functions could be derived from $[\nabla^2 + k^2]G = -\delta(\vec{x} - \vec{x}')$, with the right boundary conditions on the cell walls, instead of replicating image terms. Even the factors $J_0(ka)$ and $I_0(\Gamma_{n0}a)$, due to integrating over symmetric current distributions on the post surface, could be found by this route too. By the route we chose, each post sees the same $\epsilon_0{}^i$, which includes scattering contributions from all the others, so the mutual interactions of post and images will be included in an $\epsilon_0{}^s$ based on the terms with $n = 0$ in G.

The scattered fields for both structures are derived in Appendix IV from $A_y = \mu \int_0^b G(y, y_0)\, I(y_0)\, dy_0$. Variational forms arise from $\int_0^b \epsilon(y) I(y)\, dy = 0$, as for a single PLF post, but the impedance $Z_0 = -\epsilon_0{}^s/I_0$ is changed by image effects:

$$Z_0(wg) = \frac{\zeta kb}{\kappa w} J_0(ka) \sin \frac{\pi x_0}{w} \sin \frac{\pi}{w}(x_0 + a) \cdot (1 + j \cot \epsilon(wg)) \quad (35)$$

$$Z_0(sl) = \frac{\zeta b}{2w} J_0(ka)(1 + j \cot \epsilon(sl)). \quad (36)$$

Here $\cot \epsilon = \mathrm{Im}\,(Z_0)/\mathrm{Re}\,(Z_0)$ plays the role of $\cot \delta_0$ for an isolated post, and is given by a series like Lewin's equation [3, eq. 11], or Marcuvitz's equation [5, sec. 5.11, p. 256, eq. 1]:

$$\cot \epsilon(wg) = \sum_{m=2}^{\infty} \frac{\kappa}{\Gamma_{0m}}\left\{\frac{\sin m\pi x_0/w \sin m\pi(x_0+a)/w}{\sin \pi x_0/w \sin \pi(x_0+a)/w}\right\} \quad (37)$$

$$\cot \epsilon(sl) = \sum_{m=1}^{\infty} \frac{k}{\Gamma_{0m}}[\cos m\pi a/w + \cos m\pi(2x_0+a)/w]. \quad (38)$$

Because we can retain $G(n)$, Z_n remains the same as in (9) and $q(u)$ in (19) is unchanged, but Y_0 will be given by $1/Z_0$, (35) or (36); with this change, and with ϵ replacing δ_0, the circle and line equations (21) and (22) apply now to scatter from a post in waveguide or in stripline.

IX. Correlation with Marcuvitz's Data

Marcuvitz's data, although taken before 1950 and printed without analysis, are at least readily available. The data consist of values of X_a and X_b, as noted in Section II above, for a centered post in X-band guide (0.9 in × 0.4 in). They are given in three sets for posts of radius 1/32 in (I), 1/16 in (II), and 1/8 in (III); in each set three frequencies, corresponding to λ (free space) of 3.4, 3.2, and 3.0 cm, were used, and a selec-

[1] Evanescent modes ($n \geq 1$) from sources in other cells make a very small addition to A_y in the main cell, if $\Gamma_{n0}w > 2$, so $K_0(\Gamma_{n0}a) \gg K_0(\Gamma_{n0}2mw)$.

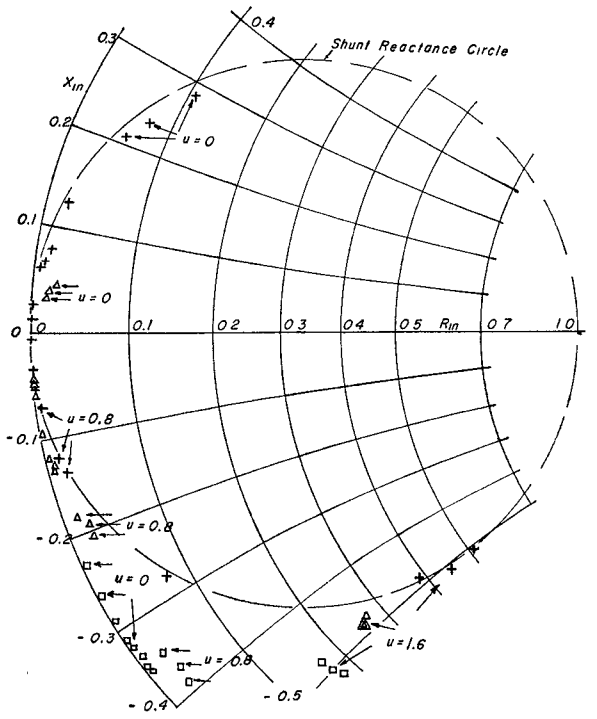

Fig. 6. Marcuvitz's data, converted to a normalized input impedance $Z_{in}=R_{in}+jX_{in}$, seen looking at a post backed by a matched load and plotted on the Smith chart. Key: $+a=1/32$ in; $\Delta a=1/16$ in; $\square a=1/8$ in.

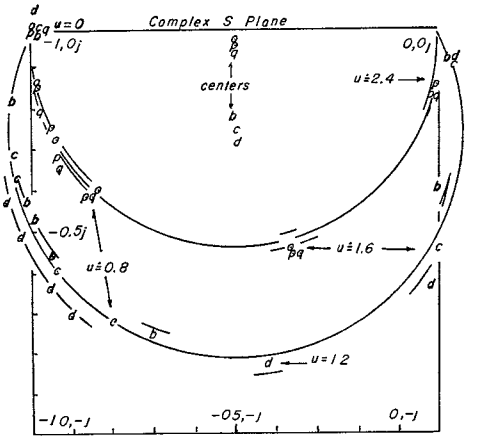

Fig. 7. On the plane of complex scattering S, two sets of data from Fig. 6 are replotted; points bcd are for a post of 1/32-in radius, points opq are for one of 1/16-in radius and various gap widths u.

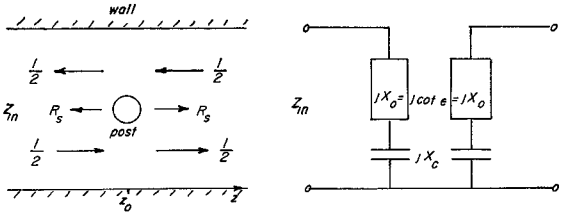

Fig. 8. Symmetric or even field excitation of a post in a waveguide and a lumped element model after Schwinger.

tion of three to six gap sizes. Analysis of these data will show how our scattering results apply, and how the gap reactance depends on gap size and post radius.

To start on familiar ground, we plot $Z_{in}(X_a, X_b)$, the normalized impedance seen looking at the post backed by a matched load, on a section of the Smith chart in Fig. 6:

$$Z_{in} = j(X_a - X_b)\,(1 - W) + W,$$
$$W \equiv X_a^2\,[1 + (X_a - X_b)^2]^{-1}. \quad (39)$$

Data sets I(+) and II(Δ) fall on or close to the dashed circle $R=-(1+2jX)^{-1}$. In set III(□) the points fall below this circle and show the importance in Z_{in} of the series term X_b. The reflection R of a traveling wave passing a lossless element with simple shunt reactance X falls on this circle for any X in $(-\infty<X<\infty)$. The values of u indicate gap width; the frequency variation within each set (<14 percent) is not coded.

We replot data sets I and II on the S plane in Fig. 7, using the relations:

$$\frac{Z_{in}-1}{Z_{in}+1} = R = \frac{E_y^s}{E_y^i} \qquad R(1+j\cot\epsilon) = S = \frac{\epsilon_0{}^s}{\epsilon_0{}^i}. \quad (40)^2$$

Fig. 7 illustrates the S equations (21) and (22) and serves to contrast S, the $(n=0)$ field ratio at the post surface, with R of Fig. 6, the wave-field ratio at large $|z-z_0|$. Since cot ϵ depends on frequency (or ka) and fixes the center of the S circle, Fig. 7 also spreads the points: set I points (bcd) have $ka=0.147$, 0.156, and 0.166, respectively, while set II points (opq) have ka values double these. To avoid cluttering Fig. 7, only one complete circle is drawn for each set. The value of cot ϵ may be taken from the data (for a post with no gap, $S=-1$) or calculated from (37); here agreement was good.

To include data of set III in further analysis, the reflection R of Fig. 6, from one traveling wave, must be distinguished from R_s, the reflection under symmetric excitation or even fields. Opposite traveling waves of $\frac{1}{2}$ unit amplitude, incident from left and right in Fig. 8, may give an even unit field at the post. The waves pass through the post, and the post, asserting its boundary conditions, radiates a reflection R_s both ways. At a plane $\mathcal{K}|z-z_0|=n\pi$ to the left of the post,

$$Z_{in} = \frac{\overrightarrow{(1/2)} + \overleftarrow{(1/2+R_s)}}{\overrightarrow{(1/2)} - \overleftarrow{(1/2+R_s)}} = \frac{1+R_s}{-R_s} = Z_{11} + Z_{12}$$
$$= j(2X_a - X_b). \quad (41)$$

To find the gap reactance X_c, we first insert $Z_0=\text{Re}\,(Z_0)\cdot(1+j\cot\epsilon)$ and $S=R_s(1+j\cot\epsilon)$ into (19) to obtain

$$1 + \frac{1}{R_s} + j\{\cot\epsilon - [8ka\eta\ \text{Re}\,(Z_0)q(u)]^{-1}\} = 0. \quad (42)$$

In this expression one can identify the reactance of a post with no gap, $X_0=\cot\epsilon=(2X_a-X_b)\,|_{u=0}$, and X_c, the deviation from X_0 caused by the gap:

$$X_c = [8ka\eta\ \text{Re}\,(Z_0)q(u)]^{-1} = \Delta(2X_a - X_b). \quad (43)$$

For thin posts, $R=R_s$, and the shunt reactance of a thin post with gap is $X=\frac{1}{2}(X_0-X_c)$.

Solving for $q(u)$ in (42) we plot the data points, including set III, in Fig. 9 as $q(u)=[8ka\eta\ \text{Re}\,(Z_0)\ X_c]^{-1}$. The dashed curve q_r was found by variational methods [(30) and Appen-

[2] At large $|z-z_0|$ only the imaginary part of $G(wg)$ from (33) contributes to $E_y{}^s$, so $E_y{}^s b=-I_0\ \text{Re}\,(Z_0)$; for a centered post $E_y{}^i=\mathcal{E}_0{}^i$; by definition $Z_0I_0=-\mathcal{E}_0{}^s b$.

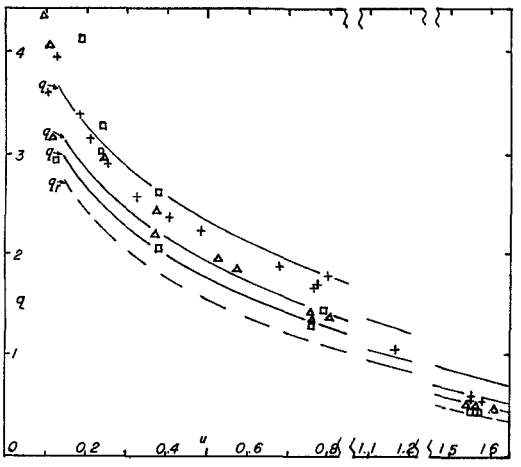

Fig. 9. The gap reactance function $q(u)$ as calculated from (44) in the solid curves and as found for the point sets I, II, and III from the data in the *Waveguide Handbook*. Key: $+a=1/32$ in; $\Delta a=1/16$ in; $\square a=1/8$ in.

dix III] in zero order, i.e., uniform gap field and no adjustable constants:

$$q_r(u) = 2Q_2(2u)[(2u)^{-2}] = 0.807 - \ln|u| + u^2/36 + \cdots. \quad (44)$$

The solid curves give $q(u)$ corrected: $Y_1{}^a$ of (18) is a poor estimate for the first modal admittance, $Y_1{}^e$ of (9):

$$q(u) = q_r + (\epsilon_1/\epsilon_0{}^t)^2\left[\frac{Y_1{}^e - Y_1{}^a}{4jka\eta}\right]. \quad (45)$$

Here, in zero order, $\epsilon_1/\epsilon_0{}^t=(\sin u)/u$. The correction for Y_2 proved negligible. The data points fall along the solid curves with some scattering. Lewin [3] predicted the logarithmic trend of $q(u)$ as $u\to 0$, which the data points also show.

Eisenhart and Khan in [7, fig. 22] plot $X_{\text{obs}}{}'$ against frequency, and a reviewer requested this format for Fig. 9. The gaps used by Marcuvitz differ from run to run, however, so his data must be plotted against u. In the limited range of frequency explored ($\Delta f/f\sim 13$ percent), $P(f)\equiv 8ka\eta$ Re (Z_0) is near a minimum, and varies with f less than 1 percent: $P_{\text{I}}=0.768$ for set I, $P_{\text{II}}=1.485$, and $P_{\text{III}}=2.56$; the near doubling of P from set to set reflects mainly the doubling of the post radius a. We plot $q(u)$ in Fig. 9, therefore, without coding frequency. Readers who wish to visualize results in terms of $1/X_c$ may multiply $q(u)$ by this factor P.

X. Further Discussion of Lewin's Papers

In Lewin's 1957 paper, the gap is also the input to a coaxial line; it experiences "a voltage drop Z_1I when a current flows at the end of the probe," and the "field at the stub surface is $Z_1I\,\delta(x)$" [3, p. 110]. Changing Lewin's x to our y, we may take $Z_1I\,\delta(y)$ as the limit of $-(V/d)h(d-y)$ as $d\to 0$, a common form in antenna work [16]. Lewin's equation [3, eq. (3)], relating the gap field to the field scattered there by $I(y)$ on the post, is an assumption about the form of $\epsilon(y)$. When Lewin "solves" for $I(y)$ in [3, eq. (13)–(20)], he makes its Fourier expansion consistent with $\epsilon(y)$. If $\epsilon(y)$ be the trial function, it belongs in a variational form for $\epsilon(y)$, our (30); such apparently is Lewin's equation [3, eq. (23)], although he started with a form variational in $I(y)$ like our (31).

The series $\sum_{n=1}^{\infty} 1/jX_n$ in Lewin's equations [3, eq. (18)–(23)] diverges wildly. If it represents $\sum_{n=1}^{\infty} Y_n|\epsilon_n|^2/|\epsilon_0{}^t|^2$, the divergence can be blamed in part, as Lewin suggests, on allowing the "turns-ratio" for a uniform field $\epsilon_n/\epsilon_0{}^t=(\sin nu)/nu$ to become 1 as his gap vanishes. But the divergence is also due to the form X_n [3, eq. (10)], and he suggests stopping the sum at $n=b/2a$ when the lack of the factor $I_0(\Gamma_{n0}a)$ becomes disturbing. This factor in our Y_n protects our sum in (30) from divergence, and was obtained through boundary conditions on fields inside our fictitious cylinder of current. [The actual current density depends on r as $J_0(-\sqrt{j\omega\mu\sigma}r)$, a cumbersome form which all models avoid.] Lewin, in proposing the similar factor exp $(\Gamma_{n0}a)$, also considers relations in the post between his fictitious axial current filament and the post surface.[3] In his 1959 paper [4], Lewin gives in cylindrical coordinates the evanescent fields near an isolated post; he includes effects of a current sheet and a visible gap in his model, thus improving his 1957 paper in several ways. He does not, however, reconcile the 1959 and 1957 results or put the post back in the waveguide as we have done.

Lewin's fifteen-year-old problem with divergences should challenge others to supply a firmer analysis, yet several more recent papers [10], [17], and [18] use his waveguide results without improving X_n. Collin [19] also treats the probe antenna in a waveguide, integrating over a product of Green's function and J, "currents on the probe and aperture surface" [19, p. 258]. Four pages later he allows the current to shrink to a filament. Thus as with Lewin, $I_0(\Gamma_{n0}a)=1$, but Collin keeps to a form variational in current. Thus for his Z_n, the sum $\sum_{n=1}^{\infty} Z_n|I_n|^2/|I_0|^2$ no doubt converges too fast, but no series in $1/Z_n$ arises, and no divergence problem either.

XI. Lines for Further Work

Lumped equivalent circuits often help in systematic interpretation of microwave data, as for instance, Tsai, Rosenbaum, and MacKenzie [20] demonstrate for the post, but one needs an adequate field theory, even for this simple geometry, to develop circuit parameters [21] and to know how far to trust a given circuit. For a post in multimode guide one needs a field theory of a round model rather than a strip [7]. Thus our discussion of scattering from a post, and a companion discussion of the driven gap, should be extended to include odd excitation of thick posts, and multimode excitation.

Criticism in microwave field theory has a distinguished tradition; for example, Bouwkamp [22] found a hole in Bethe's famous paper on small coupling holes [23], and Wigner [24] found an omission in Slater's expansion on cavity mode fields [25]. The gap between Lewin's two influential treatments of a post with gap was in part clear to Lewin; I hope I have filled it in.

Appendix I

Symbols used in two or more sections are listed alphabetically as follows, with the Section (in parentheses) in which the symbol first occurs.

a, b, d	Post and gap dimensions (II and Fig. 1).
A_y	Vector potential component (III).

[3] Certain statements in [3, sec. 4, pp. 112–113] seem to me to involve the θ dependence of the incident field, although Lewin writes me that they do not. Gutmann and Mortenson [10] in a parallel discussion justify stopping the sum at $n=b/a$ by a need to account for higher modes in the gap. Neither the consideration of θ variation nor of higher gap modes seems to me central to the divergence of $\sum_{n=1}^{\infty} 1/jX_n$; neither consideration is a trustworthy guide to correcting it.

A_0, A_2	Constants in the series for $q(u)$ (VI).
b, w	Waveguide dimensions (VIII).
$\epsilon(y)$	Electric field at $r=a$ (post surface) (III).
ϵ', ϵ''	Versions of $\epsilon(y)$ (V).
ϵ_i, ϵ^s	Incident and scattered parts of $\epsilon(y)$ (III).
ϵ_0, ϵ_n	Fourier amplitudes of $\epsilon(y)$ (III).
E_0, a, b, c	Constants in the expansion of $\epsilon(y)$ (V).
E^s, H^s	Field components scattered away from the post (III).
G, G_0	Green's functions for an isolated post (III).
$G(wg)$, $G(sl)$	Green's functions for a post in guide or comb (VIII).
$G(n)$	Sum of modes $n \geq 1$ in G_0 (VIII).
H_0, I_0, J_0, N_0, K_0	Standard notation for Bessel functions, always given with variable, thus $I_0(\Gamma_{n0}a)$ (II).
$I(y)$	Post current (III).
I_0, I_n	Fourier amplitudes of $I(y)$ (III).
$k=\omega/c$	Phase constant of plane wave (II).
$q(u)$	Gap reactance function (VI).
$Q_i(u)$	Clausen series (IX and Appendix III).
r, θ, y	Coordinates on the post (II and Fig. 1).
$S=s+jt$	Ratio of scattered to incident fields on the post (II).
u	Normalized gap width (V).
$\bar{u}$	Normalized distance along post axis (III).
X_a, X_b	Reactances in Marcuvitz's T circuit (II).
X_c, X_0	Post reactance elements under symmetric fields (IX).
x, y, z	Waveguide coordinates (II and Figs. 1 and 5).
x_0, z_0	Position of post axis in guide (VIII).
Y_0, Y_n	Modal admittances of isolated post (IV).
Z_0, Z_n	Modal impedances of isolated post (III).
$Z_0(wg)$	Fundamental modal impedance in guide for a post (VIII).
δ_n	Phase of Hankel function $H_n(ka)$ (II).
Γ_{n0}	Mode constant on an isolated post (III).
Γ_{0m}	Evanescent mode constant in waveguide (VIII).
ϵ	Phase of $Z_0(wg)$ (VIII).
$\mathcal{K}$	Wave constant of TE_{10} propagating mode (VIII).
$\zeta=1/\eta$	Impedance of free space (III).
$\omega=2\pi c/\lambda$	Angular frequency (II).

Appendix II

For a unit y-directed current source at $\vec{x}'$, causing a y-directed vector potential at $\vec{x}$ between parallel metal plates at $y=0$ and $y=b$, the complete Green's function is $G(\vec{r}, \vec{r}'; y, y')$:

$$G = -\frac{j}{4b} H_0(k|\vec{r}-\vec{r}'|) + \frac{1}{\pi b}\sum_{n=1}^{\infty} K_0(\Gamma_{n0}|\vec{r}-\vec{r}'|) \cdot \cos\frac{n\pi y}{b}\cos\frac{n\pi y'}{b}. \quad (46)$$

Addition theorems for the H_0 and K_0 above yield explicit forms:

$$H_0 = H_0(kr_>)J_0(kr_<) + 2\sum_{m=1}^{\infty}\cos m(\theta-\theta')H_m(kr_>)J_m(kr_<) \quad (47)$$

$$K_0 = K_0(\Gamma_{n0}r_>)I_0(\Gamma_{n0}r_<) + 2\sum_{m=1}^{\infty}\cos m(\theta-\theta')K_m(\Gamma_{n0}r_>)I_m(\Gamma_{n0}r_<). \quad (48)$$

Appendix III

Collin [19, p. 576] outlines a technique which others might use to advantage (for instance, Eisenhart and Khan [7, p. 711]) for replacing slowly convergent Fourier series with rapidly convergent power series related to Clausen's integral [14].

1) To use this method with $\epsilon(y)$ we define $f_i(\bar{u}, u)$ thus:

$$f_{i+1}(\bar{u}, u) = \int_0^u f_i(\bar{u}, w)\,dw$$

$$f_0(\bar{u}, u) = \sum_{n=1}^{\infty}\cos n\bar{u}\cos nu. \quad (49)$$

We find $f_1 = \sum_{n=1}^{\infty}(1/n)\cos n\bar{u}\sin nu$, $f_2 = \sum_{n=1}^{\infty}(1/n)^2\cos n\bar{u}(1-\cos nu)$, and $f_3 = \sum_{n=1}^{\infty}(1/n)^3\cos n\bar{u}(nu-\sin nu)$; two of these are well known by other symbols, $(\pi/2)\delta(u-\bar{u}) = \frac{1}{2} + f_0(\bar{u}, u)$ and $h(u-\bar{u}) = (u/\pi) + (2/\pi)f_1(\bar{u}, u)$:

$$\bar{u}h(u-\bar{u}) = u + 2[f_1 - f_2/u]$$

$$\bar{u}^2h(u-\bar{u}) = 2\pi\left[\frac{u}{6} + f_1 - \frac{2f_2}{u} + \frac{2f_3}{u^2}\right]. \quad (50)$$

2) On dividing each nth Fourier term in f_i by n, we obtain g_i; for instance, $g_0(\bar{u}, u) = \sum_{n=1}^{\infty}(1/n)\cos n\bar{u}\cos nu$. In fact

$$g_0 = \sum_{n=1}^{\infty}\frac{1}{2n}[\cos n(\bar{u}+u) + \cos n(\bar{u}-u)] = -\tfrac{1}{2}[\ln 2|\cos u - \cos\bar{u}|] \quad (51)$$

as in (27), but the g_i for $i \geq 1$ do not have closed forms. Simpler forms Q_i, defined like f_i by iteration of integrals, are useful to express g_i; thus with $Q_{i+1}(u) = \int_0^u Q_i(w)\,dw$, we find

$$Q_0(u) = \sum_{n=1}^{\infty}\frac{1}{n}\cos nu = -\ln\left[2\sin\frac{u}{2}\right] = -\ln|u| + \frac{u^2}{24} + \frac{u^4}{1440} + \cdots$$

$$Q_1(u) = u[1 - \ln|u|] + \frac{u^3}{72} + \cdots$$

$$Q_2(u) = \frac{u^2}{2}\left[\frac{3}{2} - \ln|u|\right] + \frac{u^4}{288} + \cdots$$

$$Q_3(u) = \frac{u^3}{6}\left[\frac{11}{6} - \ln|u|\right] + \frac{u^5}{1440} + \cdots = \sum_{n=1}^{\infty}\left[\frac{1}{n}\right]^4[nu - \sin nu]. \quad (52)$$

In terms of Q's, the functions $g_i(u, u)$ plotted in Fig. 10 are

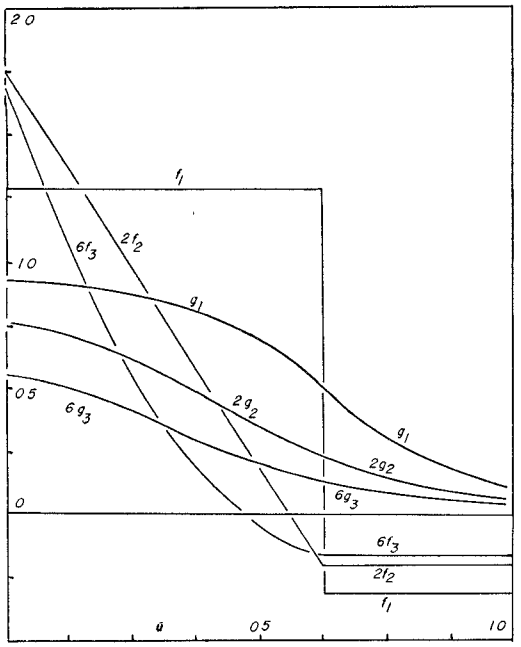

Fig. 10. The gap field functions $f_i(u)$ and the post current functions $g_i(u)$ near the gap, which give the basis for Fig. 4.

$$g_1 = \tfrac{1}{2}[Q_1(u+\bar{u}) + Q_1(u-\bar{u})]$$
$$g_2 = \tfrac{1}{2}[Q_2(u+\bar{u}) + Q_2(u-\bar{u})] - Q_2(\bar{u})$$
$$g_3 = \tfrac{1}{2}[Q_3(u+\bar{u}) + Q_3(u-\bar{u})] - uQ_2(\bar{u}). \quad (53)$$

3) If $\epsilon(y)$ is given in terms of f_1, f_2, and f_3, then $I(y)$ can be expressed with g_1, g_2, and g_3. Thus as plotted in Fig. 4,

$$\epsilon''(y) = \frac{E_0 u}{\pi}\left[1 + b + \frac{c}{6}\right] + \frac{2E_0}{\pi}\left[f_1 + b(f_1 - f_2/u) + c\left(f_1 - \frac{2f_2}{u} + \frac{2f_3}{u^2}\right)\right] \quad (54)$$

$$I''(y) = I_0 - 8jka\eta E_0 \frac{b}{\pi}\left[g_1 + b(g_1 - g_2/u) + c\left(g_1 - \frac{2g_2}{u} + \frac{2g_3}{u^2}\right)\right]. \quad (55)$$

When $\epsilon(y)$ and $I(y)$ are given by such forms, the integral which defines $q(u)$ in (30), $\int_0^b e(y)\, i(y)\, dy$, consists of terms of the form $\int_0^\pi f_i g_j\, d\bar{u}$ which integrate to give $Q_{i+j}(2u)$. For example, from (43), $\int_0^\pi f_1 g_1\, d\bar{u} = 2\, Q_2(2u)[(2u)^{-2}]$. Here we have an accurate form for the whole "tail" ($n \to \infty$) of the Fourier series for $q(u)$, although we may still need to correct the "front end" ($n = 1$) as in (44) if $Y_1^a \neq Y_1^e$.

Appendix IV

Forms based on Poisson's summation [19, p. 588] will allow us to include neatly the image sources for the fields.

1) Whenever the Fourier transform of $f(b)$, $F(\tau) = \int_{-\infty}^{\infty} f(b) \exp -jb\tau\, db$ exists, it follows that $\sum_{n=-\infty}^{\infty} f(\alpha n) = (1/\alpha)\sum_{p=-\infty}^{\infty} F(2\pi p/\alpha)$. The transforms we need are [19, p. 268]:

$$\int_{-\infty}^{\infty} \exp j\tau b H_0(y\sqrt{a^2+b^2})\, db = 2j \exp\{-a\sqrt{\tau^2 - y^2}\}\{\sqrt{\tau^2 - y^2}\}^{-1} \quad (56)$$

$$\int_{-\infty}^{\infty} \exp j\tau b K_0(y\sqrt{a^2+b^2})\, db = \pi \exp\{-a\sqrt{\tau^2+y^2}\}\{\tau^2+y^2\}^{-1/2}. \quad (57)$$

Now let $b = x - x_0 + q$, $db = dq$, $a = z - z_0$, and $y = k$; then pass to discrete forms $\tau \to 2\pi p/\alpha = \pi p/w$ and $q \to 2mw = \alpha m$. One finds

$$\sum_{m=-\infty}^{\infty} H_0(k\sqrt{(z-z_0)^2 + (x - x_0 + 2mw)^2}$$
$$= \frac{j}{w}\sum_{p=-\infty}^{\infty}\frac{1}{\Gamma_{0p}}\exp\left\{\frac{-j\pi p}{w}(x - x_0) - \Gamma_{0p}|z - z_0|\right\}$$
$$= \frac{1}{kw}\exp\{-jk|z - z_0|\} + \frac{2j}{w}\sum_{p=1}^{\infty}\frac{1}{\Gamma_{0p}}\cos\frac{\pi p}{w}(x - x_0)\exp\{-\Gamma_{0p}|z - z_0|\}. \quad (58)$$

Lewin [3] uses the similar sum over

$$K_0(\Gamma_{n0}\sqrt{(z-z_0)^2 + (x - x_0 + 2mw)^2}).$$

2) In the waveguide, $E_y^{\text{inc}} = E^i \sin(\pi x/w) \exp -j\kappa z$ and $H_x^{\text{inc}} = (\eta\kappa/k)E_y^{\text{inc}}$; we follow Lewin in choosing on the post the surface point $z = z_0$, $x = x_0 + a$, at which to evaluate the scattered field component ϵ_0^s. At a reasonable distance from the post E_y^s consists only of the first term below times $\exp -j\kappa|z - z_0|$; the terms with $m \geq 2$ are each attenuated by a factor $\exp\{-\Gamma_{0m}|z - z_0|\}$:

$$\epsilon_0^s = -\frac{\zeta k}{\kappa w} J_0(ka) I_0 \left\{\sin\frac{\pi x_0}{w}\sin\frac{\pi(x_0 + a)}{w} + j\sum_{m=2}^{\infty}\frac{\kappa}{\Gamma_{0m}}\sin\frac{m\pi(x_0 + a)}{w}\sin\frac{m\pi x_0}{w}\right\}. \quad (59)$$

3) For a stripline similarly, at a reasonable distance, the first term below times $\exp\{-jk|z - z_0|\}$ alone survives in E_y^s:

$$\epsilon_0^s = -\frac{\zeta}{2w} I_0 J_0(ka) \cdot \left\{1 + j\sum_{m=1}^{\infty}\frac{k}{\Gamma_{0m}}\left[\cos\frac{m\pi a}{w} + \cos\frac{2m\pi x_0}{w}\right]\right\}. \quad (60)$$

H_x^s may be found from E_y^s, and then $Z_0(sl)$ as in Section III.

Acknowledgment

The author wishes to thank Dr. R. Gutmann and Dr. K. Mortenson for pointing out Lewin's work.

References

[1] L. Infeld, "The impedance of a rectangular waveguide with a thin antenna," *Can. J. Res. Sect. A*, vol. 27A, pp. 109–129, July 1949.
[2] L. Lewin, *Advanced Theory of Waveguides*. London, England: Iliffe, 1951, ch. 4.1, pp. 76–88.
[3] ——, "A contribution to the theory of probes in waveguides," *Inst. Elec. Eng. Mono.* 259R, Oct. 1957.
[4] ——, "A contribution to the theory of cylindrical antennas—Radiation between parallel plates," *IRE Trans. Antennas Propagat.*, vol. AP-7, pp. 162–168, Apr. 1959.
[5] N. Marcuvitz, Ed., *Waveguide Handbook*. New York: McGraw-Hill, 1951, pp. 271–272.

[6] J. A. Bradshaw, "The current on a post driven from a gap," *IEEE Trans. Microwave Theory Tech.*, to be published.
[7] R. L. Eisenhart and P. J. Khan, "Theoretical and experimental analysis of a waveguide mounting structure," *IEEE Trans. Microwave Theory Tech.*, vol. MTT-19, pp. 706–719, Aug. 1971.
[8] P. Morse and H. Feshback, *Methods of Theoretical Physics*, vol. II. New York: McGraw-Hill, 1953, pp. 1377–1379 and 1564.
[9] J. Schwinger and D. Saxon, *Discontinuities in Waveguides*. New York: Gordon and Breach, 1968, pp. 44–46 and 72.
[10] R. J. Gutmann and K. E. Mortenson, "An ordered array of terminated metallic posts as an embedding network for lumped microwave devices," *IEEE Trans. Microwave Theory Tech.*, vol. MTT-20, pp. 215–223, Mar. 1972.
[11] C. T. Tai, *Dyadic Green's Functions in Electromagnetic Theory*. Scranton, Pa.: International Book, 1971, pp. 69–100.
[12] L. F. Jelsma, E. D. Tweed, R. L. Phillips, and R. W. Taylor, "Boundary conditions for the four vector potential," *IEEE Trans. Microwave Theory Tech.* (Corresp.), vol. MTT-18, pp. 648–649, Sept. 1970.
[13] V. H. Rumsey, "Reaction concept in electromagnetic theory," *Phys. Rev.*, vol. 94, p. 1484, June 15, 1954.
[14] M. Abramowitz and I. Stegun, *Handbook of Mathematical Functions* (Applied Mathematics Series 55). Washington D. C.: NBS, 1964, p. 1005.
[15] R. W. P. King, *The Theory of Linear Antennas*. Cambridge, Mass.: Harvard Univ. Press, 1956, pp. 122.
[16] ——, *The Theory of Linear Antennas*. Cambridge, Mass.: Harvard Univ. Press, 1956, p. 70.
[17] D. C. Hanson and J. E. Rowe, "Microwave circuit characteristics of bulk GaAs oscillators," *IEEE Trans. Electron Devices (Second Special Issue on Semiconductor Bulk Effect and Transit-Time Devices)*, vol. ED-14, pp. 469–476, Sept. 1967.
[18] J. Scanlon and M. Kodali, "Characteristics of waveguide-mounted tunnel diodes," *Proc. Inst. Elec. Eng.*, vol. 114, pp. 1844–1849, Dec. 1967.
[19] R. E. Collin, *Field Theory of Guided Waves*. New York: McGraw-Hill, 1960, pp. 258–271 and Appendix A.6, pp. 576–589.
[20] W. C. Tsai, F. J. Rosenbaum, and L. A. MacKenzie, "Circuit analysis of waveguide-cavity Gunn-effect oscillator," *IEEE Trans. Microwave Theory Tech. (Special Issue on Microwave Circuit Aspects of Avalanche-Diode and Transferred Electron Devices)*, vol. MTT-18, pp. 808–817, Nov. 1970.
[21] S. P. Yu and J. D. Young, "Measurement of interaction impedance of microwave circuits for solid-state devices," *IEEE Trans. Microwave Theory Tech.* (Corresp.), vol. MTT-18, pp. 999–1001, Nov. 1970.
[22] C. W. Bouwkamp, "On Bethe's theory of diffraction by small holes," *Phillips Res. Rep.*, vol. 5, pp. 321–332, Oct. 1950.
[23] H. A. Bethe, "Theory of diffraction by small holes," *Phys. Rev.*, vol. 66, pp. 163–182, Oct. 1944.
[24] T. Teichmann and E. Wigner, "Electromagnetic field expansions in loss-free cavities excited through holes," *J. Appl. Phys.*, vol. 24, pp. 262–267, Mar. 1953.
[25] J. C. Slater, *Microwave Electronics*. New York: Van Nostrand, 1950, ch. IV and V, pp. 57–101.

Gain–Bandwidth Limitations of Microwave Transistor Amplifiers

RODNEY S. TUCKER

Abstract—**Gain–bandwidth limitations of broad-band single-stage microwave transistor amplifiers are related to a simple transistor circuit model, to constraints on characteristic impedance in a distributed-element equalizer, and to the line lengths of this equalizer. The gain–bandwidth performance of commensurate distributed-element equalizers is compared with the performance of a lumped-element equalizer, and four distributed-element design examples are presented, including two commensurate equalizers and two computer-optimized networks.**

I. Introduction

STIMULATED by developments in microwave transistor technology, a number of authors have discussed the problem of broad-band microwave transistor amplifier design using computer-aided techniques [1], [2]. Recently, the work on broad-band impedance matching introduced by Fano [3], and extended by Youla [4] and other authors, has been applied to the synthesis of distributed commensurate equalizers for microwave transistor amplifiers [5]. This procedure relies upon certain approximate models of the transistor, but has proved successful in the design of single-stage and multistage amplifiers and in the problem of choosing an appropriate design with which to begin a computer-aided optimization scheme.

Manuscript received July 10, 1972; revised December 11, 1972. This work was supported by the Australian Radio Research Board.

The author is with the Department of Electrical Engineering, University of Melbourne, Parkville, Victoria, Australia.

This paper extends the scope of work previously reported [5]. In Section II the gain–bandwidth limitations of a single-stage amplifier are related to a simple transistor circuit model, to constraints on the characteristic impedance in a distributed-element equalizer, and to the line lengths of this equalizer. The gain–bandwidth performance of commensurate distributed equalizers is compared with the performance of a lumped-element equalizer. In Section III it is shown that techniques introduced by Levy [6] for the synthesis of a ladder network with stub lengths different from those of the interconnecting lines may be used to advantage, this being illustrated in Section IV by an equalizer of improved gain–bandwidth performance. Gain–bandwidth limitations for a particular transistor are estimated in Section IV and some design examples are presented using both the direct synthesis method and a computer-aided technique. Theoretical and experimental results are compared.

II. Limitations on Amplifer Gain

The study of gain–bandwidth properties of a microwave transistor amplifier requires a suitable representation of transistor performance at frequencies approaching f_{max}, the maximum frequency of oscillation. Complex circuit models have been proposed [9], but are not readily suited to the problem. The work in this paper relies upon both an analytic or numerical model of transistor gain and a simple circuit model representing the output impedance of the transistor.